International Journal of Nanomedicine

Dovepress
open access to scientific and medical research

Open Access Full Text Article

ORIGINAL RESEARCH

Modified FGF Hydrogel for Effective Axon Formation by Enhanced Regeneration of Myelin Sheath of Schwann Cells Using Rat Model

Jiandong Li[1,2,*], Zhitao Shangguan[1,2,*], Xiaoqing Ye[1,2], Zhenyu Wang[1,2], Wenge Liu[1,2], Gang Chen[1,2]

[1]Department of Orthopaedics, Fujian Medical University Union Hospital, Fuzhou, China; [2]Union Clinical College, Fujian Medical University, Fuzhou, China

*These authors contributed equally to this work

Correspondence: Gang Chen; Wenge Liu, Tel +86-15880004731; +86-13705977551, Email xiehechengang0591@fjmu.edu.cn; wengeunion@fjmu.edu.cn

Introduction: An acute spinal cord injury (SCI) is a debilitating event for which there is no targeted or effective treatment. Previous studies have shown that fibroblast growth factor (bFGF) and Schwann cells (SC) exert a protective effect on the injured tissues. Because of their easy injectability and strength, hydrogels are considered to be ideal candidates for creating loadable tissues. However, the application and mechanism of bFGF-hydrogels have not been explored.

Methods: We synthesized a new class of bFGF-hydrosol and evaluated its safety and biocompatibility in vitro and in vivo. Next, an SCI rat model was established to evaluate the effect of the hydrosol on an SCI by detecting various pro-inflammatory markers and evaluating the injury. The ability of hydrosol to promote axon formation was evaluated by detecting corresponding indexes, and its ability to promote remyelination was evaluated by detecting the corresponding indexes in Schwann cells.

Results: A novel in situ injectable hydrogel containing bFGF (HA-bFGF) was synthesized and found to have better biocompatibility than other gels. HA-bFGF helped to repair tissue damage after an SCI in vivo. Our mechanistic investigation also showed that HA-bFGF improved axon formation after an SCI by facilitating the regeneration of myelin sheath of Schwann cells.

Conclusion: In this study, we found that HA-bFGF could promote neural restoration and tissue recovery after an SCI. Our results indicate that hydrogels loaded with bFGF can alleviate a spinal cord injury by promoting the remyelination of Schwann cells, reducing inflammation at the injured site, and ultimately promoting axon generation.

Keywords: acute spinal cord injury, HA-bFGF, Schwann cells

Introduction

A spinal cord injury (SCI) is a serious medical event that can lead to severe sensory and motor dysfunction. Axonal growth and functional recovery after a spinal cord injury are limited because adult central nervous system neurons are less naturally regenerative, and various biological and environmental factors such as inflammation, myelin-associated inhibitors, glial scar components, chondroitin sulfate, or a decreased blood supply can impair axonal recovery and growth.[1–3] Previous attempts to treat spinal cord injuries by targeting extrinsic mechanisms that control axonal regeneration have met with limited success.[4,5] Furthermore, removal of extracellular inhibitory molecules, attempts at neurotrophy delivery, and permitted substrate transplantation have not resulted in a robust regeneration and substantial recovery of function in damaged axons. There remains a need to develop appropriate interventions that can improve the serious consequences of a spinal injury.

In recent years, the multiple functions of angiogenic factors such as basic fibroblast growth factor growth factor (bFGF) have been identified in neurons and neuroglia. Among those angiogenic factors, bFGF has been reported to be useful in treating ischemia after an injury and to exert neurostimulatory effects on the developing and adult nervous systems of mice and other mammals.[6–10] Exogenous bFGF implantation or overexpression of bFGF in mesenchymal stem cells might be an effective method for preserving spinal cord tissue, reducing degeneration, improving blood vessels, and reducing the

Received: 5 May 2023
Accepted: 9 November 2023
Published: 5 December 2023

numbers of apoptotic cells.[11,12] Therefore, we developed a protocol designed to promote the targeted release of bFGF. This protocol can more accurately deliver bFGF to the intended target area and improve tissue regeneration after an SCI.

Hydrogels are very soft and wet materials that have received a great amount of attention by members of the biomedical engineering community due to their extracellular matrix structure and composition.[13–15] Because of their injectability and high strength, hydrogels have been identified as ideal candidates for creating load-bearing tissues in patients requiring minimal or non-invasive therapy; for example, patients who require cartilage regeneration or bone defect repair.[16–18] However, the combined use of bFGF and an injectable hydrogel in treatment of an SCI has not been previously explored.

In this study, we synthesized a novel bFGF-modified hydrogel (Figure 1A and B) and examined its biocompatibility. We also assessed and compared the anti-inflammatory effects of hydrogels with bFGF (HA-bFGF) with bFGF treatment alone in vitro, and administered HA-bFGF to an SCI animal model in vivo. We hypothesized that HA-bFGF might improve the spinal cord environment and promote axon regeneration after an acute spinal cord injury.

Materials and Methods

Synthesized Synthesis of a Novel bFGF (HA-bFGF)-Modified Hydrogel

Briefly, 0.1 g of hyaluronic acid (HA) powder was dissolved in 10 mL of ultrapure water to obtain a 10 mg/mL solution. After adjusting the pH value to 4, 29.14 mg of SNHS (N-hydroxy sulfosuccinimide activated hyaluronic acid) solution

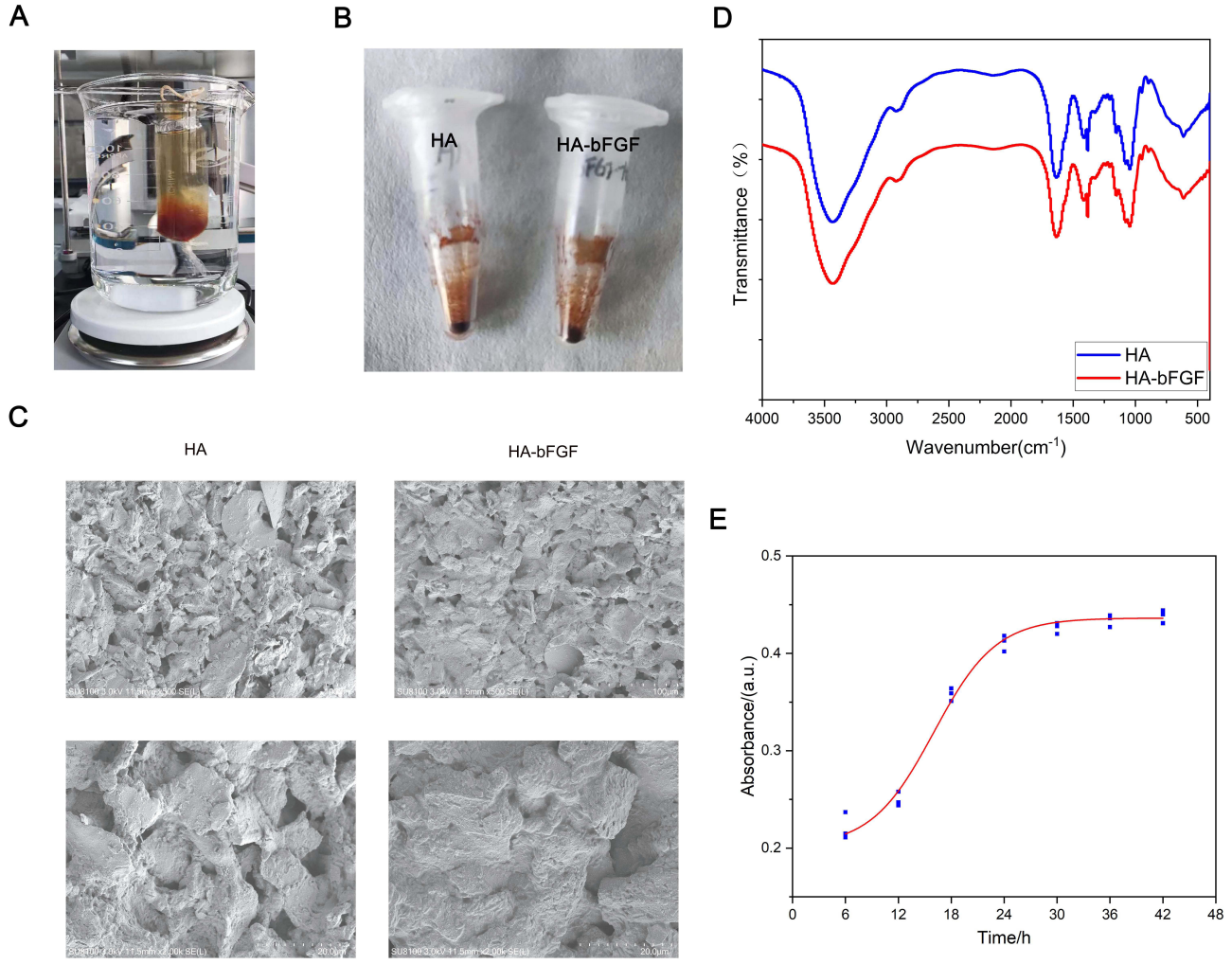

Figure 1 Synthesis of HA-bFGF hydrogel. (**A**) The process of synthesis. (**B**) The appearance of the finished product. (**C**) The morphological structure of HA-bFGF hydrogel and HA hydrogel as detected by SEM. (**D**) FTIR spectra of HA and HA-bFGF. (**E**) HA-bFGF drug release curve.

and 48.53 mg of EDC were added under agitation, and the reaction was allowed to proceed at room temperature for 3 hours. Next, the pH of the solution was adjusted to 7.4 to stop the reaction and HA-sNHS was obtained. The reaction products were purified with ethanol and then dialyzed with ultrapure water at 4°C through a seamless cellulose tube (cut-off molecular weight, 8000) for 5 days, with the ultrapure water being replaced on a daily basis. HA-bFGF hydrogel was prepared by adding 2 μg of bFGF to the hydrogel solution, stirring the solution at a low temperature until the hydrogel fully dissolved, and then letting the solution stand at 4°C for 24 hours. Finally, the purified polymer was freeze-dried in a vacuum freeze-dryer and designated as HA-sNHS.

Characterization

The HA-bFGF was incubated in phosphate buffer at 37°C for periods of 6, 12, 18, 24, 30, 36, and 42 h. Next, the solutions were collected and placed in a multifunctional microplate reader that recorded their absorbance values at 280 nm, which reflected the release concentrations of the materials. Microscopic surface morphology was detected using a HITACHI Regulus 8100 Scanning Electron Microscope (SEM) system. The chemical structure and functional groups of HA and HA-bFGF were characterized by their Fourier transform infrared (FTIR) spectra, which were obtained using a Nicolet Avatar 360 FTIR system with KBr disks. The spectra were collected over the range of 400–4000 cm^{-1}.

Spinal Cord Injury Using Rat Model

The animal experimentations in the study were reviewed and approved by the ethical committee of Fujian Medical University and all animal experiments were conducted in accordance with welfare guidelines for experimental animals promulgated by the People's Republic of China: Laboratory animals - General Code of Animal Welfare (GB/T 42011–2022). To ensure complete anesthesia during surgery, the adult female Sprague-Dawley rats (200–250 g) used in the study received an intraperitoneal injection of ketamine (60–90 mg/kg) and a mixture of thiothiazide (10–15 mg/kg) in combination with inhalation of 1–2% isoflurane. After lifting the spinal cord with a spinal hook, the spinal cord was transected at the T10 level using a microshear device. To fully observe and verify the integrity of the lesion, we raised the severed stump so that the string passed through the gap to ensure the absence of any residual fibers on the bottom and side of the tube.

Behavioral Analysis

Motor Recovery Assessments and scoring were performed by blinded investigators using the Basso, Betty, and Bresnahan (BBB) motor rating scale methods. Measurements were taken as baseline scores every 2–3 days after implantation, and then on a weekly basis. Sensory recovery was assessed using the von Frey filament test. A fiber with a bending force gradient (Bioseb, North Pinellas Park, FL, USA) was applied to the claw to initiate a nociceptive response (rapid claw withdrawal from stimulation). The withdrawal threshold was defined as the minimum force needed to induce a positive response in at least 2 of 3 trials, with a trial interval of at least 30 seconds.

Cell Viability Assay

Cell viability was analyzed using the MTT assay. Briefly, cells were cultured in 96-well plates (2500 cells/well) for 24 h. After 72 h, cell viability was determined by the $OD_{450\ nm}$ value recorded when using a CCK-8 (no. HY-K0301, MCE, NJ, USA) kit, according to manufacturer's instructions.

Western Blot (WB) Assay

Samples of protein were separated by SDS-PAGE, and the protein bands were transferred onto PVDF membranes (number 03010040001, Sigma-Aldrich, St. Louis, MO, USA), which were subsequently blocked with TBS in 5% milk. Next, the membranes were incubated overnight with a primary antibody at 4°C, followed by incubation with an HRP-conjugated secondary antibody. Immunostaining of protein bands was detected using a chemiluminescence reagent, photographed using a ChemiDoc IRS system (Bio-Rad, Hercules, CA, USA), and quantified using Image J software.

Nissl Staining

On days 14 and 28 after creation of a SCI, 3 rats from each group were randomly selected to receive an intraperitoneal injection of ketamine (60–90 mg/kg) and a mixture of thiothiazide (10–15 mg/kg) in combination with inhalation of 1–2% isoflurane. Next, samples spinal cord tissue were fixed, dehydrated, paraffin embedded, and sectioned. After dewaxing, the tissue sections were stained with 1% toluidine blue for 40 min, washed with distilled water, and dehydrated with a graded alcohol series (70%, 80%, and 95%, and 100% ethanol). After treatment with xylene, the sections were sealed with neutral gum and photographed under a light microscope.

H&E Staining

For H&E staining, the sections were dewaxed and then stained with hematoxylin for 10–20 sec; after which, they were washed in distilled water and then stained with eosin for 1–3 min. After additional washing with distilled water, the sections were sequentially submerged in 95% alcohol I solution for 5 min, 95% alcohol II solution for 5 min, absolute ethanol for I.5 min, absolute ethanol II solution for 5 min, xylene I solution for 5 min, and xylene II solution for 5 min to produce transparency. The tissue sections were then gently dried, sealed with neutral gum, and examined and photographed under a light microscope.

Immunofluorescence (IF) Assay

Tissues on confocal dishes were fixed with 4% paraformaldehyde for 20 min at room temperature, permeabilized using 0.5% Triton X-100 in PBS, and blocked with 3% goat serum for 1 h at 37°C. The cells were then incubated overnight with primary antibodies at 4°C, followed by incubation with fluorogenic secondary antibodies at room temperature for 1 h. Cell nuclei were stained with DAPI for 2 min. Images were acquired with a Confocal microscope (ZEISS, Oberkochen, Germany).

Histology

Tissue specimens were fixed in 10% buffered formalin for 24 h, and then embedded with paraffin. Next, tissue sections (5 μm thickness) were obtained and histology assays were performed by a senior pathologist.

Statistical Analysis

All statistical data were analyzed using GraphPad PRISM 7.0 software, and results are presented as a mean value ± S.D. Mean differences between two or more groups were compared using Student's *t*-test or analysis of variance (ANOVA). A P-value < 0.05 was considered to be statistically significant.

Results

Micromorphology of HA-bFGF Hydrogel and Biocompatibility Testing in vitro and vivo

The cross-sectional morphology of the new hydrogel was observed by scanning electron microscopy (SEM) to judge the condition of the hydrogel. The results showed that the hydrogels with or without BFGF had a reticular porous network structure. At low magnification, a dense tubular cavity with different diameters of interconnected pores was observed in the HA and HA-bFGF gels, but the pores in the HA-bFGF group were smaller and more rounded (Figure 1C). To obtain a more intuitive evaluation, we used high power microscopy, and the results showed that HA-bFGF had smaller and more numerous pores when compared with the HA control group (Figure 1C). These findings indicated that the HA-bFGF had been successfully prepared and met the requirements of quality control. HA-bFGFHA-bFGFWe used then used FTIR spectroscopy to investigate the roles of HA and HA-bFGF in a spinal cord injury. The results showed that the FTIR spectra of HA and HA-bFGF had similar peaks at the same point (Figure 1D). In addition, in order to explore the sustained release effect of the bFGF in HA-bFGF, we used an experimental microplate reader to measure the absorbance of the leachate of HA-bFGF at 260 nm HA-bFGFat different time points (Figure 1E). Those results showed that bFGF release reached its maximum level at between 24 h and 30 h, indicating the uniformity of drug release.

To fully evaluate the safety (or toxicity) and biocompatibility HA-bFGF in cells, we first conducted imaging studies to observe cell morphology with or without HA-bFGF treatment, and found that HA-bFGF had no obvious effect on cell morphology (Figure 2A). We then investigated the effects of HA-bFGF on cell proliferation and found that HA-bFGF had no impact on cell proliferation, which was similar to the bFGF group (Figure 2B). At the same time, we used the ELISA method to measure the levels of lactate dehydrogenase (LDH) in cells to judge the functional integrity of cell secretion as an indication of cell toxicity. The results showed that the HA-bFGF group was similar to the bFGF and HA groups, as the LDH levels in all of the groups were not affected (Figure 2C). Finally, we examined the biocompatibility of HA-bFGF in mice and evaluated the effects of HA-bFGF on the heart, liver, spleen, lung, and kidney by H&E staining. The results showed that HA-bFGF had no toxicity to these organs, and was relatively safe (Figure 2D). Taken together, these results indicated superior biocompatibility of the HA-bFGF hydrogel.

HA-bFGF Helped to Repair Injury to the Spinal Cord in Rats

To evaluate the neuroprotective potential of HA-bFGF in treatment of an SCI, a rat model of SCI was established. The time span we chose to observe was 2–3 h after the injury was created. This is because the routine procedure used in clinical treatment is to initiate hydrogel treatment at 2 hours after the SCI to achieve neuroprotection and functional recovery. After treatment, the rats were assessed with the BBB exercise score every week for 4 weeks. The results showed that a 7-day period of HA-bFGF treatment significantly improved exercise recovery in the SCII rats when compared with all other treatment groups (Figure 3A).

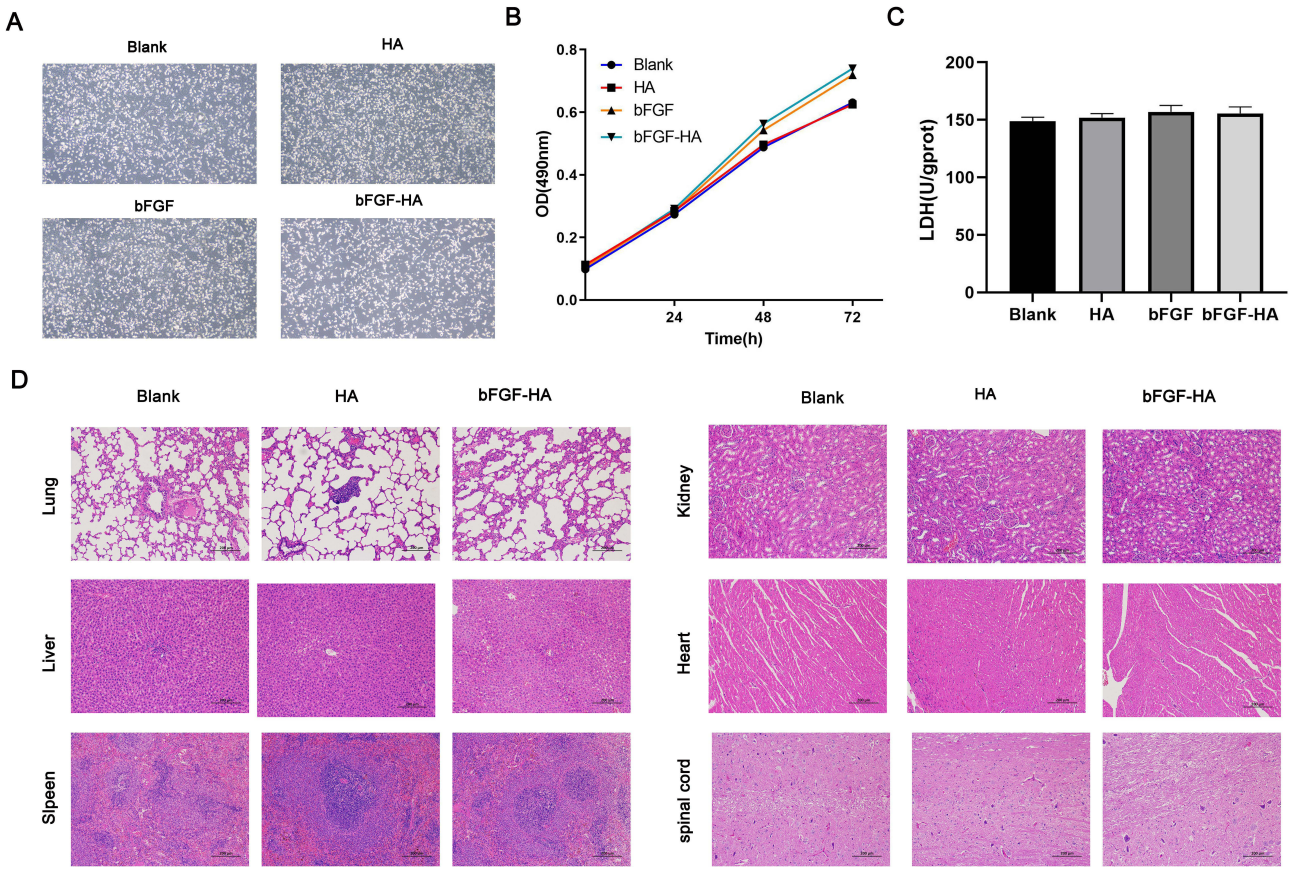

Figure 2 In vitro and in vivo biocompatibility testing of HA-bFGF hydrogel. (**A**) The morphological structure of neuroglial cells in the 4 groups. (**B**) MTT assays were performed to measure cell proliferation. OD values at 490 nm were determined at 0 h, 24 h, 48 h, and 72 h after drug administration. (**C**) ELISA assays were used to detect LDH activity. (**D**) Biocompatibility testing in vivo. HA and HA-bFGF were injected into rats in the different experimental groups. H&E staining was used to detect morphological changes in sections of heart, liver, lung, kidney, and spleen tissue.

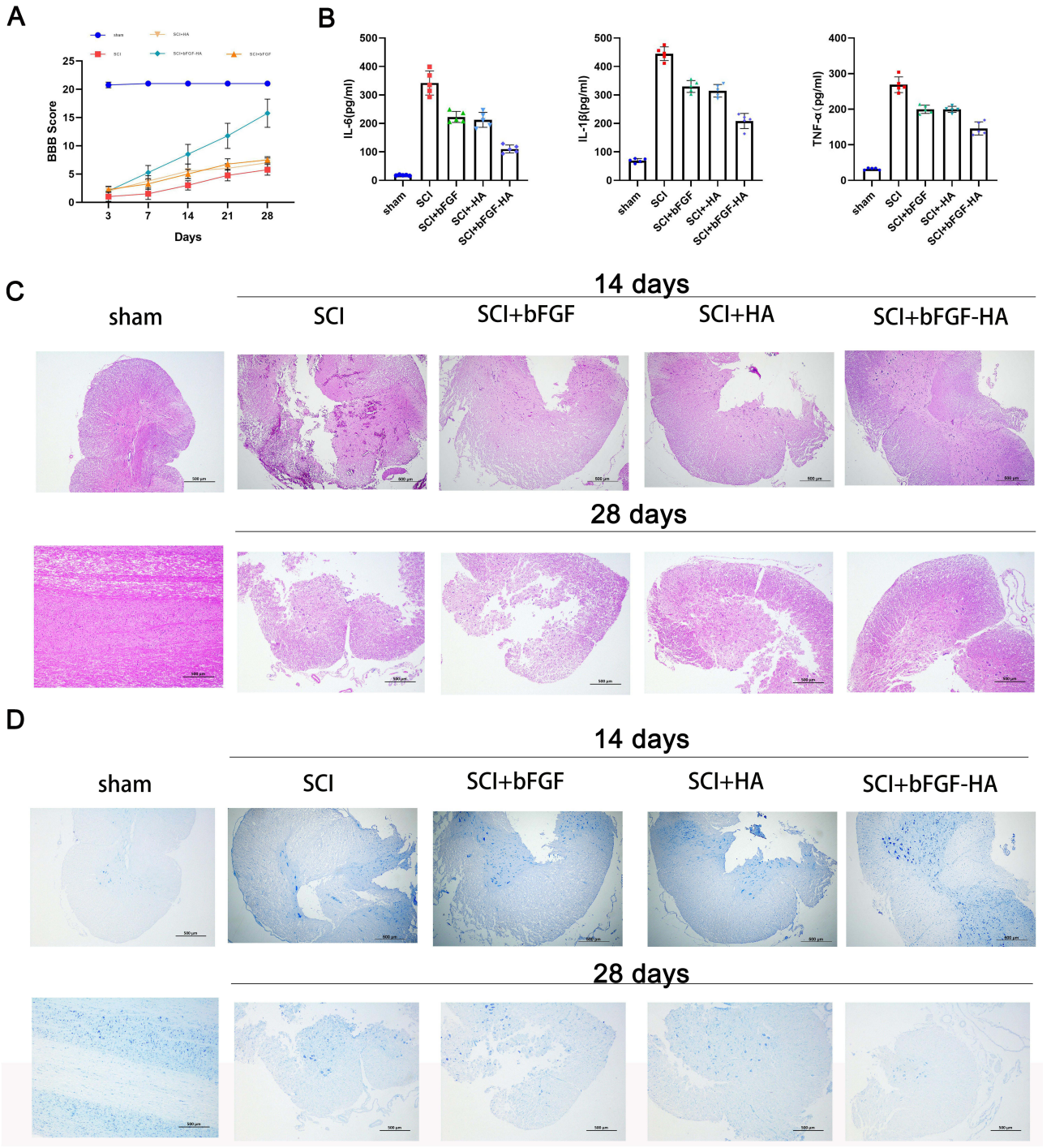

Figure 3 HA-bFGF hydrogel helped to repair spinal cord injuries in rats. (**A**) Spinal cord injury severity was evaluated by the BBB score at 3, 7, 14, 21, and 28 days after hydrogel administration. (**B**) The expression of inflammatory factors (IL-6, IL-1β, and TNF-α) in blood samples from rats in the different groups was examined by ELISA. (**C**) After 14 and 28 days of treatment, samples of injured spinal cord tissue were removed, stained with H&E, and examined under a microscope. (**D**) After 14 and 28 days of treatment, samples of injured spinal cord tissue were removed, subjected to Nissl staining, and examined under a microscope. Size bar, 500 μm.

To evaluate the ability of HA-bFGF to block inflammation, the levels of proinflammatory factors (IL-6, IL-1β and TNF-α) were detected by ELISA. HA-bFGFAs shown in Figure 3B, the levels of IL-6, IL-1β, and TNF-α in rat serum were elevated after the SCI; however, they were significantly reduced after treatment with HA-bFGF, indicating that HA-bFGF could reduce the levels of proinflammatory factors (Figure 3B). These data suggest that HA-bFGF treatment played a role in reducing inflammation after the SCI.

Next, we investigated axonal regeneration in the SCI rats by examining the condition of the spinal cord after injury. Our results showed that an injured rat spinal cord that did not receive intervention had obvious intercellular spaces in the cell-segregating domain. The three different intervention groups (HA, BFGF, and HA-bFGF) showed different levels of tissue regeneration, with the HA-bFGF group showing the highest degree of regeneration (Figure 3C). A comparison of H&E staining results at 14 days and 28 days showed that the severity of the SCI increased with time. However, the spinal cord showed some repair in the treatment groups, and the HA-bFGF group showed the highest amount of repair. Notably, in the HA-bFGF group, erythrocytes could be observed in the lumen, indicating that the vasculature had begun to develop after the SCI. We also examined the levels of Nissl in tissues to account for the exercise recovery capacity after injury, and the results showed that exercise recovery was clearly best in the HA-bFGF Group (Figure 3D). An SCI leads to a decrease in the number and deformation of Nissosome bodies, which is more prominent after 28 days. The number of Nithrosome bodies in the HA-bFGF group was significantly higher at 28 days than at 14 days. These results suggest that HA-bFGF has the ability to maintain nerve repair and tissue recovery after a spinal cord injury.

HA-bFGF Improved Axon Formation After a Spinal Cord Injury

Because HA-bFGF showed an ability to dramatically improve the anatomical appearance of an injured spinal cord, we investigated whether HA-bFGF affected axon formation at 14 days and 28 day after an SCI. To end this, we first examined the expression of TUBB3, which is a marker of microglial cells, and also the expression of GFAP, which is a marker of astrocytes and indicates the infiltration of microglia or astrocytes after an SCI. GFAP is also used to indicate the extent of an injury. The results showed that the numbers of microglia cells or astrocytes in the HA-bFGF-treatment group were significantly decreased (Figure 4A), indicating that HA-bFGFbFGF treatment could effectively reduce the severity of an SCI. Microglia cells can gradually migrate to the lesion core and form microglia near the inside of the astrocyte scar. The tight distribution of microglia and astrocytes suggests an interaction between those two cell types. We next examined the expression of growth associated protein 43 (GAP43) and NAF200, which are key markers of axonal regeneration and plasticity. We found that GAP43/NAF200 expression was highest in the HA-bFGF-treatment group (Figure 4B), indicating that HA-bFGF promotes axonal formation after an SCI. Moreover, Schwann cell survival was better in the HA-bFGF group, and Schwann cells in the HA-bFGF group also showed better migration than Schwann cells in the other groups (Figure 4C) Finally, a comparison of MBP-Nogo-A expression at 14 and 28 days showed that the numbers of Schwann cells in the HA-bFGF group increased over time.

Western blot assays for GFAP, GAP43, NAF200, MBP, and Nogo-A expression showed similar results in the SCI damage tissues (Figure 5A and B). Furthermore, the results were consistent with those of immunofluorescence experiments. The findings indicated that HA-bFGF could promote the survival of Schwann cells after an SCI, and also promote axon regeneration and inhibit the aggregation of microglia cells and astrocytes, which blocks the efficacy of SCI repair. Taken together, these results indicated that treatment with HA-bFGF could promote both spinal cord regeneration and axon regeneration, and enhance the recovery of neurological function after an SCI, while HA treatment alone had little effect on those processes.

HA-bFGF Facilitated the Regeneration of Schwann Cell Myelin Sheath

To further reveal the effects of HA-bFGF on Schwann cells in the SCI model rats, we extracted Schwann cells from the rats and then observed the morphological changes in Schwann cells by immunofluorescence assays. The results showed that b-FGF-HA could stimulate Schwann cells to produce antennae and initiate remyelination, and those effects were not as obvious in the other groups (Figure 6A). Therefore, we investigated whether b-FGF-HA could alter the expression of remyelination-related genes and thereby initiate morphological changes in Schwann cells. To this end, we performed IF assays, the results of which showed that b-FGF-HA could indeed increase MBP expression (Figure 6B) and decrease Noga-A expression (Figure 6C). Western blot assays for MBP and Nogo-A showed similar results after b-FGF-HA treatment (Figure 6D and E). These data suggest that b-FGF-HA can facilitate the activation of Schwann cells and the regeneration of myelin sheath induced by LPS.

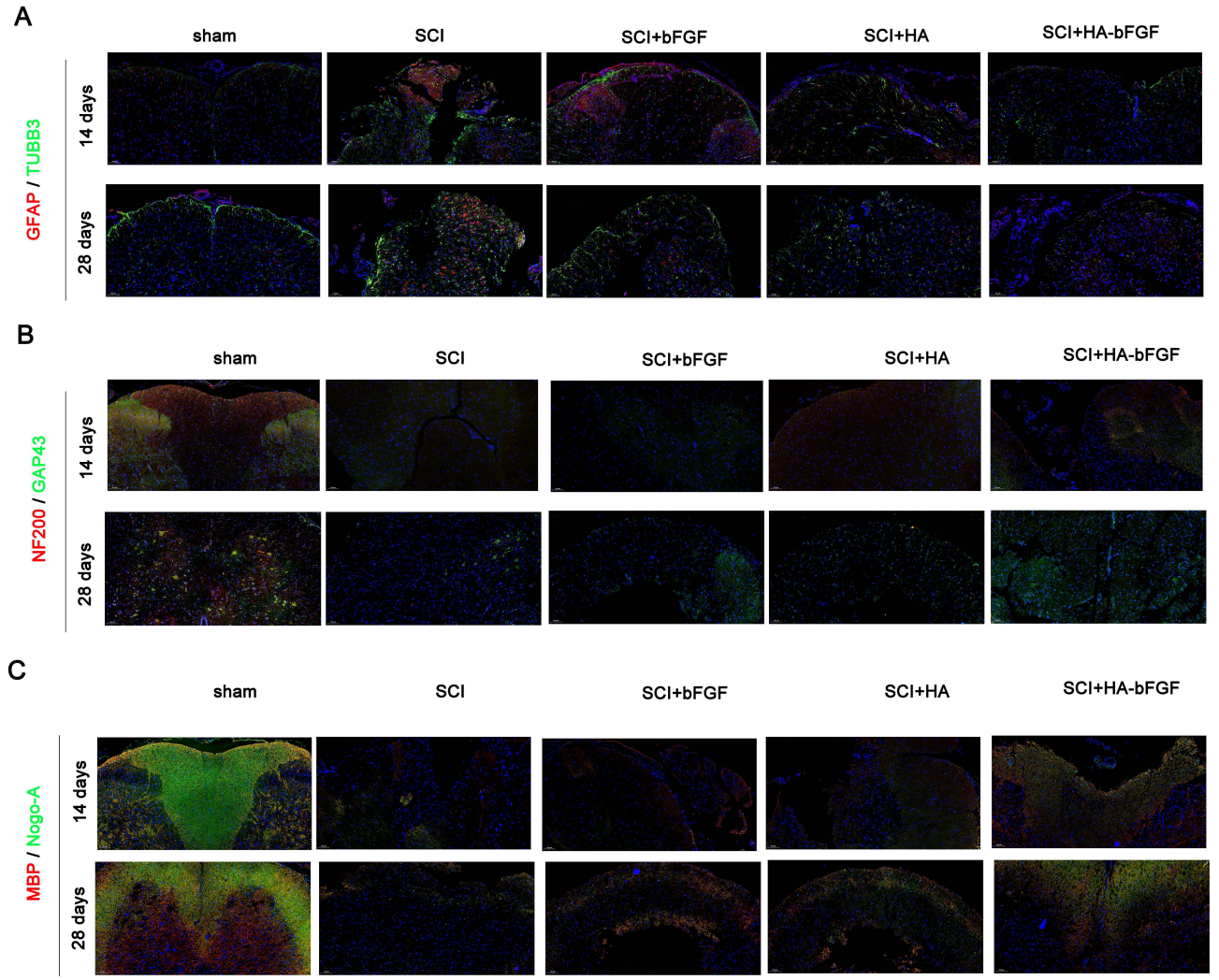

Figure 4 HA-bFGF hydrogel improved axon formation after a spinal cord injury. (**A**) The levels of TUBB3 (a marker for microglia) and GFAP (a marker for astroglia) after 14 and 28 days of treatment, respectively. (**B**) The expression of *NAF200* and *GAP43* (two marker genes for axons) and (**C**) *MBP-Nogo-A* (a marker gene for Schwann cells) after 14 and 28 days of treatment, respectively.

Discussion

Tissue destruction secondary to a spinal cord injury in humans is caused by a gradual decrease in blood flow to the spinal cord region following the injury. This decrease in blood flow leads to ischemic anoxic necrosis and a series of other biochemical events in the damaged area.[4] Eventually, the damage spreads to multiple sites, leading to the formation of microcavities and cysts (syringomyelia), both of which accelerate damage progression, make treatment more difficult, and result in morbidity and mortality.[5,19–23] Therefore, there remains a need to develop and implement a range of intervention strategies that address the mechanisms of a spinal cord injury and can improve clinical outcomes. In this study, we explored the effects of a novel material (HA-bFGF) in treatment of an SCI, and found that HA-bFGF could promote the generation of axons by Schwann cells, inhibit glial cells, and play a role in alleviating and treating an SCI.

Schwann cells are associated with tissue regeneration after an SCI.[24–26] Numerous growth factors are involved in regulating the function of Schwann cells during the injury recovery process. Angiogenic factors such as b-FGF are present in neurons and neuroglia and are associated with tissue ischemia and axonal regeneration after an SCI.[27,28] However, the function and mechanism of b-FGF in Schwann cells remain uncertain.[29] Researchers have attempted to find drugs that can treat a spinal cord injury. Ge et al found that zinc could regulate iron death via the NRF2/HO-1 pathway, reduce inflammatory infiltration at an injury site, and ultimately promote neuronal survival and reduce the severity of

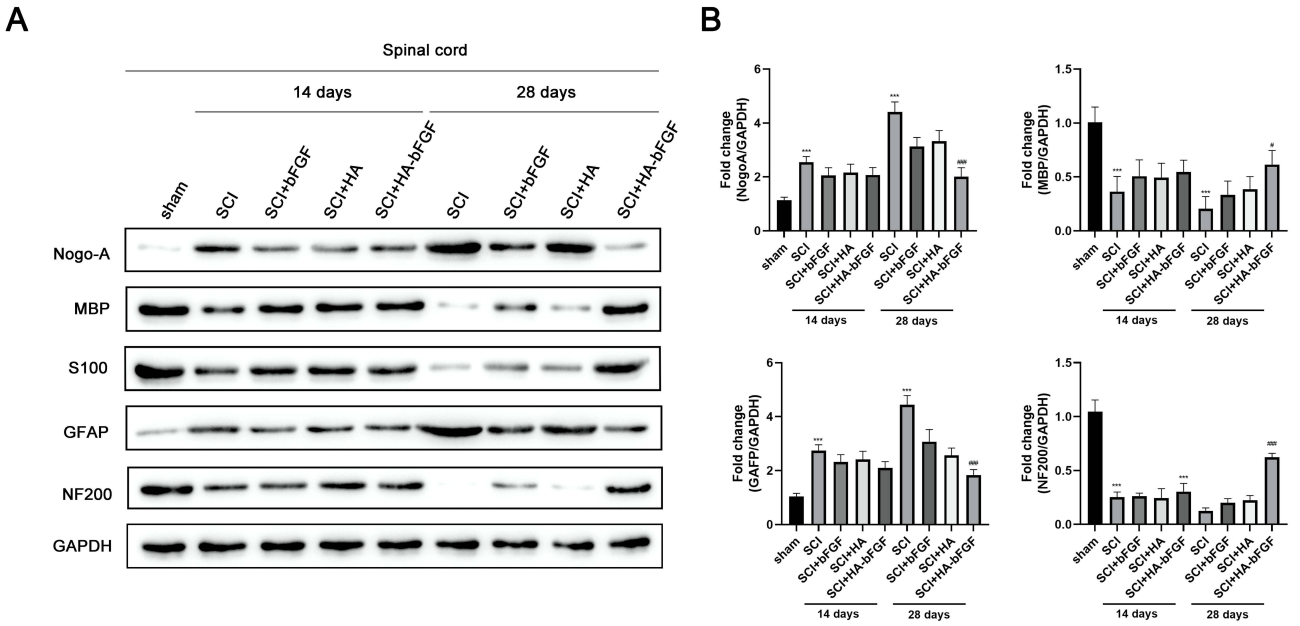

Figure 5 HA-bFGF hydrogel affected the expression of corresponding factors. (**A**) Western blot assays were performed to measure the levels of NAF200, GAP43, GFAP, and S100 expression. (**B**) A gray analysis of corresponding proteins (n = 3). ***P < 0.0001 between sham and SCI; #P<0.05, ####P<0.0001 between SCI and SCI+HA-bFGF. Size bar, 100 μm.

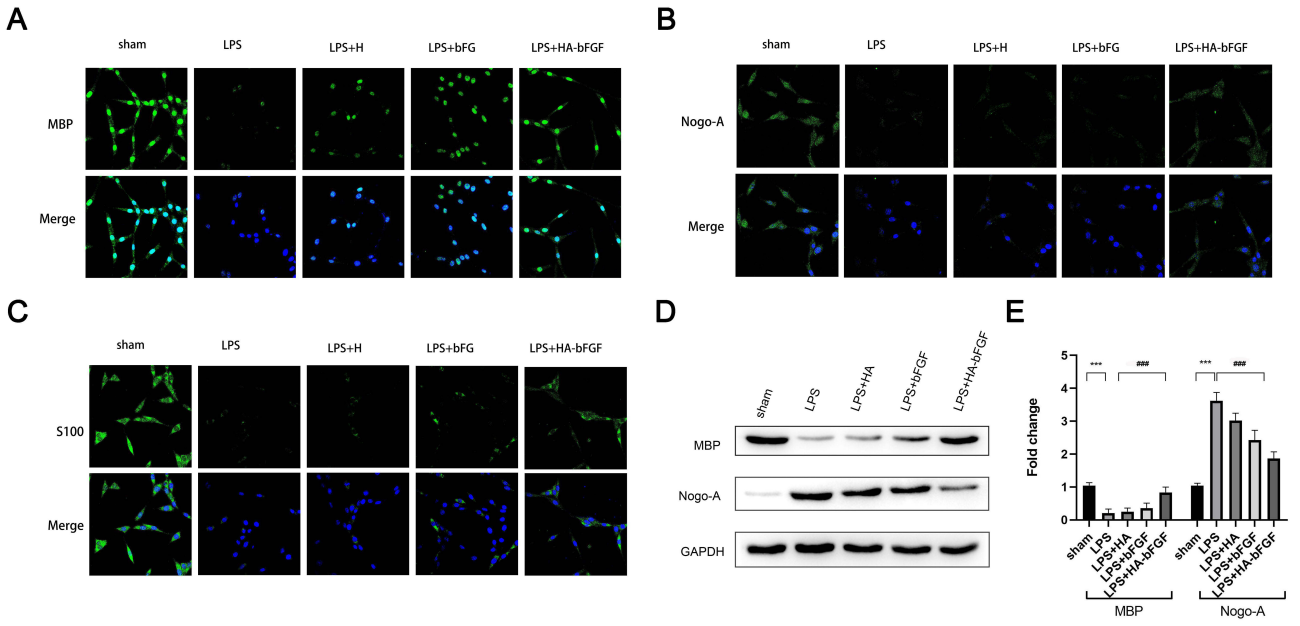

Figure 6 HA-bFGF facilitated the regeneration of myelin sheath of Schwann cells. (**A**) Immunofluorescence staining with MBP was used to detect morphological changes in cells under a confocal microscope. (**B**) Immunofluorescence assays were performed to detect the expression of Nogo-A, which influences generation of the myelin sheath. (**C**) Immunofluorescence assays were performed to detectS100 expression. (**D** and **E**) Western blot assays were performed to detect the levels of MBP and Nogo-A expression. (**D**) The representative images. (**E**) A gray analysis of MBP and Nogo-A (n = 3). ***P < 0.0001 between sham and LPS; ####P<0.0001 between LPS and LPS+HA-bFGF.

a spinal cord injury.[30] Resveratrol has been found to promote the recovery of motor function in rats after a spinal cord injury, increase the expression of brain-derived neurotrophic factors, and reduce motor neuron loss and an injury lesion size.[31] In our study, we loaded active ingredients (eg, b-FGF) onto HA and explored the ability of the newly created molecule to reduce the severity of an SCI.

Hydrogels are water-soluble three-dimensional (3D) polymer networks with adjustable physical chemistry properties.[32] As promising therapeutic agents, hydrogels have been widely used in research conducted on tissue regeneration, physiological/pathological mechanisms, and disease treatment.[33,34] With regard to biological applications, the ability of hydrogels to attach to cells can be arbitrarily adjusted by use of microfluidic strategies, and the interactions between cells and hydrogels are dynamic and relatively complex. Studies have shown that hydrogels have significant effects on physiological and pathological processes such as cell proliferation, cell migration, stem cells differentiation, and apoptosis.[35–37] Furthermore, hydrogels with in situ gel properties are suitable for subcutaneous injection in animal experiments.[38,39] Taken together, these characteristics make hydrogels of great convenience for use in studying biological systems.[32]

In this study, we synthesized a novel injectable hydrogel containing bFGF (HA-bFGF) and proved it had superior biocompatibility. We then delivered HA-bFGF to an SCI animal model in vivo. The following several lines of evidence support our observation that HA-bFGF assisted with the regeneration of myelin sheath after an SCI: 1) The HA-bFGF hydrogel had no toxicity to the organs of rats and was relatively safe, indicating a higher level of biocompatibility; HA-bFGF2) HA-bFGF markedly reduced the levels of inflammation-related biomarkers in SCI tissues; 3) HA-bFGF maintained neural restoration and tissue recovery after an SCI; 4) treatment with HA-bFGF promoted spinal cord regeneration, axon regeneration across the scar boundary, and enhanced the recovery of neurological function after an SCI; 5) b-FGF-HA facilitated the activation of Schwann cells and the regeneration of myelin sheath induced by LPS.

Conclusion

In summary, we found that HA-bFGF could promote the myelin re-sheath of Schwann cells, reduce the production and infiltration of microglia and astroglia, and promote axon regeneration by neuronal cells in treatment of an SCI. HA-bFGF showed good biocompatibility and a strong therapeutic effect. The main loading material is HA, which is relatively expensive and may be an economic consideration for patients. On the other hand, Schwann cells mainly grow in the peripheral nervous system, and although their numbers are small, they also function in the spinal cord. Therefore, it is necessary to further explore the mechanism of action of Schwann cells in the spinal cord in follow-up studies. On the other hand, we used bFGF in the hydrogel for regeneration of myelin sheath, and this is a promising technique for improving repair at a spinal cord injury site. Furthermore, our mechanistic investigation showed that HA-bFGF improves axon formation at the site of a spinal cord injury by facilitating regeneration of the myelin sheath of Schwann cells. Therefore, the controlled in situ delivery of HA-bFGF may be a promising therapeutic strategy for repairing a spinal cord injury.

Funding

This work was supported by the Joint Funds for the innovation of science and Technology of Fujian province (2020Y9059) and the Fujian Province Guiding Project (2021Y0022, 2022Y0022).

Disclosure

The authors declare no conflicts of interest in this work.

References

1. Fischer I, Dulin JN, Lane MA. Transplanting neural progenitor cells to restore connectivity after spinal cord injury. *Nat Rev Neurosci*. 2020;21(7):366–383. doi:10.1038/s41583-020-0314-2
2. Angeli CA, Boakye M, Morton RA, et al. Recovery of over-ground walking after chronic motor complete spinal cord injury. *N Engl J Med*. 2018;379(13):1244–1250. doi:10.1056/NEJMoa1803588
3. Hawryluk GWJ, Mothe A, Wang J, et al. An in vivo characterization of trophic factor production following neural precursor cell or bone marrow stromal cell transplantation for spinal cord injury. *Stem Cells Dev*. 2012;21(12):2222–2238. doi:10.1089/scd.2011.0596
4. Fouad K, Popovich PG, Kopp MA, Schwab JM. The neuroanatomical–functional paradox in spinal cord injury. *Nat Rev Neurol*. 2020;17(1):53–62. doi:10.1038/s41582-020-00436-x
5. Filli L, Engmann AK, Zrner B, Weinmann O, Schwab ME. Bridging the gap: a reticulo-propriospinal detour bypassing an incomplete spinal cord injury. *Neurosci J*. 2014;34(40):13399–13410. doi:10.1523/JNEUROSCI.0701-14.2014

6. Presta M, Dell'Era P, Mitola S, et al. Fibroblast growth factor/fibroblast growth factor receptor system in angiogenesis. *Cytokine Growth Factor Rev*. 2005;16(2):159–178. doi:10.1016/j.cytogfr.2005.01.004
7. Livingston MJ, Shu S, Fan Y, et al. Tubular cells produce FGF2 via autophagy after acute kidney injury leading to fibroblast activation and renal fibrosis. *Autophagy*. 2023;19(1):256–277. doi:10.1080/15548627.2022.2072054
8. Nikolaou PE, Mylonas N, Makridakis M, et al. Cardioprotection by selective SGLT-2 inhibitors in a non-diabetic mouse model of myocardial ischemia/reperfusion injury: a class or a drug effect? *Basic Res Cardiol*. 2022;117(1):1–27. doi:10.1007/s00395-022-00934-7
9. Koketsu N, Berlove DJ, Moskowitz MA, et al. Pretreatment with intraventricular basic fibroblast growth factor decreases infarct size following focal cerebral ischemia in rats. *Ann Neurol*. 2010;35(4):451–457. doi:10.1002/ana.410350413
10. Wada K, Sugimori H, Bhide PG, Moskowitz MA, Finklestein SP. Effect of basic fibroblast growth factor treatment on brain progenitor cells after permanent focal ischemia in rats. *Stroke*. 2003;34:2722–2728. doi:10.1161/01.STR.0000094421.61917.71
11. Rabchevsky AG, Fugaccia I, Fletcher-Turner A, et al. Basic fibroblast growth factor (bFGF) enhances tissue sparing and functional recovery following moderate spinal cord injury. *J Neurotrauma*. 1999;16(9):817. doi:10.1089/neu.1999.16.817
12. Shi Q, Gao W, Han X, et al. Collagen scaffolds modified with collagen-binding bFGF promotes the neural regeneration in a rat hemisected spinal cord injury model. *Sci China Life Sci*. 2014;
13. Wang Z, Zhang Y, Yin Y, et al. High-strength and injectable supramolecular hydrogel self-assembled by monomeric nucleoside for tooth-extraction wound healing. *Adv Mater*. 2022;34:e2108300. doi:10.1002/adma.202108300
14. Wang W, Zeng Z, Xiang L, Liu C, Zeng H. Injectable self-healing hydrogel via biological environment-adaptive supramolecular assembly for gastric perforation healing. *ACS nano*. 2021;15(6):9913–9923. doi:10.1021/acsnano.1c01199
15. Tang Q, Plank TN, Zhu T, Yu H, Pei H. Self-assembly of metallo-nucleoside hydrogels for injectable materials that promote wound closure. *ACS Appl Mater Interfaces*. 2019;11(22):19743–19750. doi:10.1021/acsami.9b02265
16. Wang KY, Jin XY, Ma YH, Cai WJ, Ding J. Injectable stress relaxation gelatin-based hydrogels with positive surface charge for adsorption of aggrecan and facile cartilage tissue regeneration. *J Nanobiotechnology*. 2021;19:1–16.
17. Gao F, Xu Z, Liang Q, et al. Osteochondral regeneration with 3D-printed biodegradable high-strength supramolecular polymer reinforced-gelatin hydrogel scaffolds. *Adv Sci*. 2019;6(15):1900867. doi:10.1002/advs.201900867
18. Wang DA, Varghese S, Sharma B, et al. Multifunctional chondroitin sulphate for cartilage tissue-biomaterial integration. *Nat Mater*. 2007;6 (5):385–392. doi:10.1038/nmat1890
19. Zipser CM, Cragg JJ, Guest JD, et al. Cell-based and stem-cell-based treatments for spinal cord injury: evidence from clinical trials. *Lancet Neurology*. 2022;21(7):659–670. doi:10.1016/S1474-4422(21)00464-6
20. Freund P, Seif M, Weiskopf N, et al. MRI in traumatic spinal cord injury: from clinical assessment to neuroimaging biomarkers. *Lancet Neurology*. 2019;18(12):1123–1135. doi:10.1016/S1474-4422(19)30138-3
21. Bregman BS, Kunkel-Bagden E, Schnell L, et al. Recovery from spinal cord injury mediated by antibodies to neurite growth inhibitors. *Nature*. 1995;378(6556):498–501. doi:10.1038/378498a0
22. Janova H, Arinrad S, Balmuth E, Mitjans M, Nave KA. Microglia ablation alleviates myelin-associated catatonic signs in mice. *J Clin Invest*. 2018;128(2):734–745. doi:10.1172/JCI97032
23. Jakel S, Agirre E, Mendanha Falcão A, et al. Altered human oligodendrocyte heterogeneity in multiple sclerosis. *Nature*. 2019;566(7745):543–547. doi:10.1038/s41586-019-0903-2
24. Stavely R, Hotta R, Picard N, et al. Schwann cells in the subcutaneous adipose tissue have neurogenic potential and can be used for regenerative therapies. *Sci Transl Med*. 2022;14(646):eabl8753. doi:10.1126/scitranslmed.abl8753
25. Belavgeni A, Maremonti F, Stadtmüller M, Bornstein SR, Linkermann A. Schwann cell necroptosis in diabetic neuropathy. *Proc Natl Acad Sci*. 2022;119(17):e2204049119. doi:10.1073/pnas.2204049119
26. Susuki K, Raphael AR, Ogawa Y, et al. Schwann cell spectrins modulate peripheral nerve myelination. *Proc Natl Acad Sci U S A*. 2011;108 (19):8009–8014. doi:10.1073/pnas.1019600108
27. Varadarajan SG, Hunyara JL, Hamilton NR, Kolodkin AL, Huberman AD. Central nervous system regeneration. *Cell*. 2022;185(1):77–94. doi:10.1016/j.cell.2021.10.029
28. Lvarez Z, Kolberg-Edelbrock AN, Sasselli IR, et al. Bioactive scaffolds with enhanced supramolecular motion promote recovery from spinal cord injury. *Science*. 2021;374(6569):848–856. doi:10.1126/science.abh3602
29. Rajendran R, Bttiger G, Stadelmann C, Karnati S, Berghoff M. FGF/FGFR pathways in multiple sclerosis and in its disease models. *Cells*. 2021;10 (4):884. doi:10.3390/cells10040884
30. Ge MH, Tian H, Mao L, et al. Zinc attenuates ferroptosis and promotes functional recovery in contusion spinal cord injury by activating Nrf2/GPX4 defense pathway. *CNS Neurosci Ther*. 2021;27(9):1023–1040. doi:10.1111/cns.13657
31. Zhao H, Mei X, Yang D, Tu G. Resveratrol inhibits inflammation after spinal cord injury via SIRT-1/NF-κB signaling pathway. *Neurosci Lett*. 2021;762:136151. doi:10.1016/j.neulet.2021.136151
32. Cao H, Duan L, Zhang Y, Cao J, Zhang K. Current hydrogel advances in physicochemical and biological response-driven biomedical application diversity. *Signal Transduct Target Ther*. 2021;6(1):426. doi:10.1038/s41392-021-00830-x
33. Caliari SR, Burdick JA. A practical guide to hydrogels for cell culture. *Nat Methods*. 2016;13(5):405–414. doi:10.1038/nmeth.3839
34. Lin W, Kluzek M, Iuster N, et al. Cartilage-inspired, lipid-based boundary-lubricated hydrogels. *Science*. 2020;370:335.
35. Chaudhuri O, Gu L, Darnell M, et al. Substrate stress relaxation regulates cell spreading. *Nat Commun*. 2015;6(1):6364. doi:10.1038/ncomms7365
36. Wei Q, Young J, Holle A, Li J, Cavalcanti-Adam EA. Soft hydrogels for balancing cell proliferation and differentiation. *ACS Biomater Sci Eng*. 2020;6(8):4687–4701. doi:10.1021/acsbiomaterials.0c00854
37. Madl CM, LeSavage BL, Dewi RE, et al. Maintenance of neural progenitor cell stemness in 3D hydrogels requires matrix remodelling. *Nat Mater*. 2017;16(12):1233–1242. doi:10.1038/nmat5020
38. Ahearne M. Introduction to cell-hydrogel mechanosensing. *Inter Focus Theme Suppl J Royal Soc Interface*. 2014;4:20130038.
39. Yang B, Wei K, Loebel C, Zhang K, Bian L. Enhanced mechanosensing of cells in synthetic 3D matrix with controlled biophysical dynamics. *Nat Commun*. 2021;12(1):3514.